

Finite Element Modeling of Cylindrical Projectile Impact on Aluminum Plate

Basim M. Fadhil

Koya University/Faculty of Engineering

ABSTRACT

The subject of this study is to investigate the impact of cylindrical steel projectiles on aluminum plates using 3D –finite element modeling and compare the results with experimental and analytical ones. The model allows the determination of the residual velocities of projectile and the absorbed energies by the aluminum plate during impact event. Three different plate thicknesses and five different obliquity angles have been employed. It has been found that the target thickness and the obliquity angle play an important role on the behavior of the target and the residual velocities of the projectile. Good correlation has been found with analytical and experimental results.

Keywords: *Impac, Finite Element, Ballistic Limit*

1. INTRODUCTION

Awer and boder [1] carried out experimental study for normal and oblique impacts on aluminum plates .they conclude that the angle of impact has unimportant influence on the velocity reduction over a range on impact angles.

Normal impact by ogival-nosed projectiles on aluminum plate at velocities more than ballistic limit have been studied by Ansari and Gupta [2]

Iqbal and Sekhon [3] have investigated the response of thin metal plates subjected to impact by cylindrical and hemispherical-nosed projectiles using experimental and numerical approaches.

○A detailed survey of the mechanics of penetration of projectiles into targets have presented by Beckman and Goldsmith [4].They have provided insight into perforation mechanisms of plates subject to ballistic impact with schematics and experiment-based snap-shots.

The normal and oblique impacts on single and layered mild steel plates with jacketed hard-core projectiles have been studied experimentally by Gupta and Madhu [5].

Ansari and Gupta [6]. Based on the experimental results, they have developed an analytical model for predicting the residual velocity and ballistic limit.

Experimental and analytical studies have carried out by Thomas and Kevin for specifying the location and direction of ogive-nosed projectile at different angles in the ordnance velocity range.

An experimental study of impact projectiles on metal plates (mild steel, stainless steel and aluminum have studied by Corran, Shadbolt and Ruiz [7] an important effect of projectile mass as well as nose shape and plate thickness on penetration were found.

Borvik et al. [8] have conducted experiments on perforation of 12 mm thick steel plates by 20 mm diameter projectiles with different nose-shaped projectiles. They found an important effect of the nose shape of a projectile on both energy absorption and failure modes.

Normal and tilted impact of projectiles on composite target conducted by Fawaz, Zheng and Behdinan [9].

Kad, Schoenfeld and Burkins [10] discussed material modelling procedure for textured Ti-6Al-4V plates.

Borvik et al. [11] used 460 E steel plates in their studies and incorporated a damage parameter in themodified Johnson-Cook constitutive model; and, impact on HSLA-100 steel plates using quasi-static and temperature-independent material properties.

Lim, Shim and Ng [12] have studied numerically the penetration of twaron fabric; Tan, Lim and Cheong [13] investigated the penetration of Twaron fabric; GRP (glass fibre-reinforced plastic) plates as targets were

Considered by Nandall, Williams and Vaziri [14]; mild steel and aluminum plates were considered by Park, Yoo and Chung [15] for illustrating their optimization algorithm;

This paper presents a comparison between experimental, analytical and numerical study of oblique impact blunted steel projectiles on aluminum targets of three different thicknesses at different impact velocities.

2. ANALYTICAL ANALYSIS

The Kinetic energy of the projectile absorbed during perforation is of two Stages:

(1) Energy absorbed in shearing of a plug and (2) Energy absorbed in the plate bending.

In normal impact (shearing), the internal energy absorbed is taken as [16]

$$E_{sn} = (2\pi r_p h_o) 0.6 h_o \sigma_s \quad (1)$$

where E_{sn} is the energy absorbed in normal impact, r_p is the projectile diameter, h_o is the plate thickness, and σ_s the shearing strength of the plate material.

The energy absorbed in shearing of a plug in an oblique impact is

$$E_{so} = \frac{0.6\pi r_p (1 + \cos\beta) h_o^2 \sigma_s}{(\cos\beta)^3} \quad (2)$$

where β is the angle of obliquity.

The energy absorbed in dishing of the plate during oblique impact is evaluated by replacing the thickness of the plate, h_o with the effective thickness, $\left(\frac{h_o}{\cos\beta}\right)$ [2]

$$E_{ao} = \frac{\pi \left(\frac{h_o}{\cos\beta}\right) w_c^2 \sigma_y e^{12ar_p} (1 + 2ar_p)}{4(1 - \nu + \nu^2)^{0.5}} \quad (3)$$

where w_c is the central deflection of the plate, (a) is a constant measured from profile of the perforated Experimental results of the present study are plate and ν is the Poisson's ratio.

Now, the total energy absorbed during deformation of the plate is

$$E_{ao} = \frac{0.6\pi r_p (1 + \cos\beta) h_o^2 \sigma_s}{(\cos\beta)^3} + \frac{\pi \left(\frac{h_o}{\cos\beta}\right) w_c^2 \sigma_y e^{-2ar_p}}{4(1 - \nu + \nu^2)^{0.5}} \quad (4)$$

The equation of energy balance, then may be written as

$$\frac{1}{2} m v_i^2 = \frac{1}{2} m v_r^2 + E_{ao} \quad (5)$$

where v_r is the residual velocity of the projectile which may be written as

$$v_r = \sqrt{v_i^2 - \frac{2E_{ao}}{m}} \quad (6)$$

3. EXPERIMENTAL SETUP [6]

Hardened cylindrical steel projectiles of 12.8 mm diameter and 25.6 mm length were impacted through a pneumatic gun, at velocities ranging from ballistic limit of the plate to about 100 m/s. The pneumatic gun, designed and fabricated in house, is capable of firing projectiles of diameters up to 15 mm at varying impact velocities, up to 150 m/s. target plates of different sizes can be mounted in front of the gun barrel at any impact angle between 0° to 90°. Five different incident angles, viz... 0°, 15°, 30°, 45°, and 60°. and three plate thicknesses, viz., 0.81 mm, 1.52 mm, and 1.91 mm have been selected for this study. Plates of 255 mm diameter were cut from commercially available pure aluminum sheets. The average yield strength of aluminum plates is 110 MPa. The mass of the projectile and its hardness were 25.08 g and 58 Rc, respectively.

The velocity of the projectile before impact was measured with the help of two sets of photoemitter and diodes placed 25 mm apart at the exit of the barrel. The residual velocity of the projectile was measured with the help of two sets of thin aluminum foil screens, 50 mm apart, placed behind the target at a fixed distance. Impact and residual velocities were measured in each run with the help of a 4-channel digital storage. The profile of the deformed specimens was measured from the distal sides of the plates with the help of a dial gauge setup and is used for the determination of energy absorbed in the dishing of the plate. Experimental results thus obtained are plotted, wherein the effects of plate thickness and angle of obliquity on residual velocities and energy absorbed are discussed.

4. NUMERICAL MODELING

A 3D finite element modeling has been conducted for the impact pair with sufficient number of element to ensure highest possible degree of accuracy.

4.1 Projectile Modeling

The projectile was modeled with material in ANSYS-AUTODYN library adopting the material properties in the experimental study. Hence the properties of this hardened steel have been chosen for defining the behavior of projectile in current simulations. The projectile was assumed as rigid material model and build with solid elements. Therefore, the effect of element size on the projectile modeling is not important in terms of deformation and the residual velocity predictions. (Fig.1).

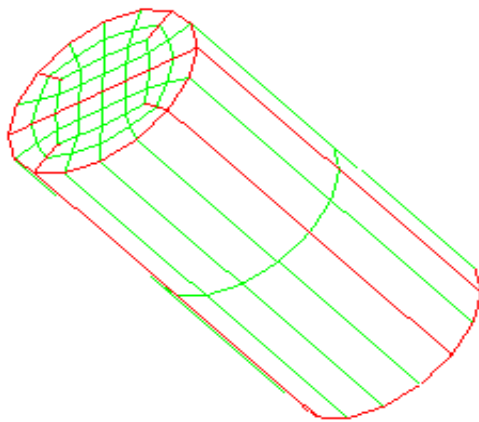


Fig. 1. Projectile modeled with solid element

4.2 Target Modeling

A finite element model of a thin aluminum plate is shown in Figures 2. The plate is circular in shape with a diameter of 255 mm and is clamped along the rim. Plates of three different thicknesses viz. 0.81 mm, 1.52 mm and 1.91 mm are considered.

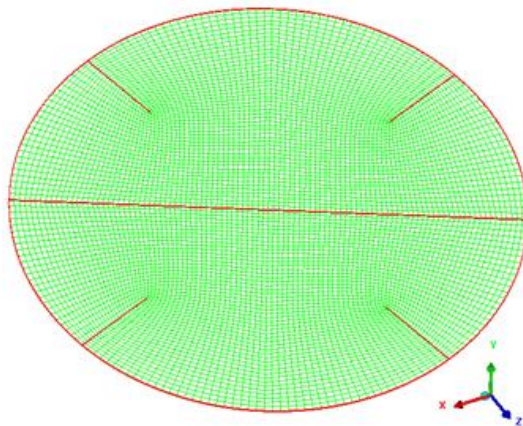


Fig. 2. Plate modeled with solid element

5. RESULTS

5.1 Ballistic Limit

Ballistic limit is an essential index for evaluating projectile and armour performance and is defined in [7] as “the average of two striking velocities, one of which is the highest velocity giving a partial penetration and the other which is the lowest velocity giving a complete penetration”. The numerical investigation ballistic limits of the plates of different thicknesses at different angles of obliquity are given in Table 1.

Table I: Ballistic Limit of Aluminum Plates of Different Thicknesses at Different Angles of Obliquity of Numerical Results

Angle of obliquity (degree)	Ballistic limit m/s of the plates		
	Plates thickness		
	h=0.81mm	h=1.52 mm	h=1.91 mm
0	35	52	63
15	30	45	60
30	28	43	59
45	38	50	65
60	50	68	85

The comparisons between the experimental and numerical results for the ballistic limit are shown in the figure 3 which shows good correlation.

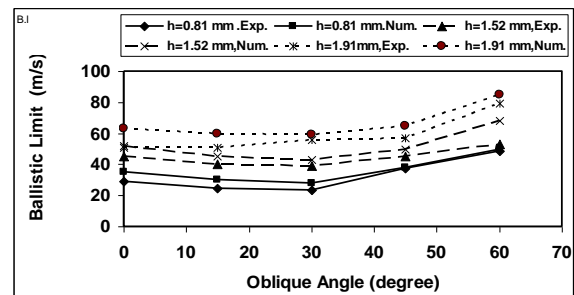


Fig3. Numerical and experimental Ballistic limit

Generally, the ballistic limit increases with increase the plate thickness where the projectile needs more kinetic energy to penetrate the plate. Also the ballistic limit is the less at the obliquity angle 30 degree where the minimum area that subjected to shear stress.

5.2 Plate Thickness Influence on The Residual Velocity (Numerical Results)

The figs. 4, 5, 6 show the computed values of residual velocity versus impact velocity for the three plate thicknesses and of different obliquity angles. Residual velocities decreases with increase obliquity angle, this effect was more clear after the angle 30 degree, besides that the obliquity angle effect increase with increase plate thickness.

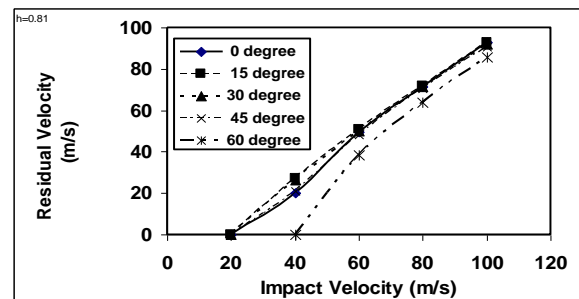


Fig.4. Residual Versus Impact Velocity For 0.81 Mm Plate Thickness With Different Obliquity Angles (Numerically)

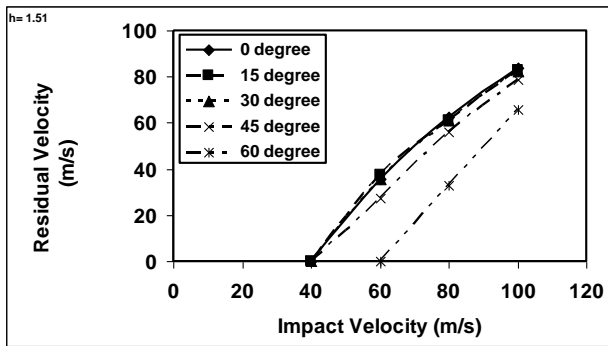


Fig.5. Residual versus impact velocity for 1.52 mm plate thickness with different obliquity angles (numerically)

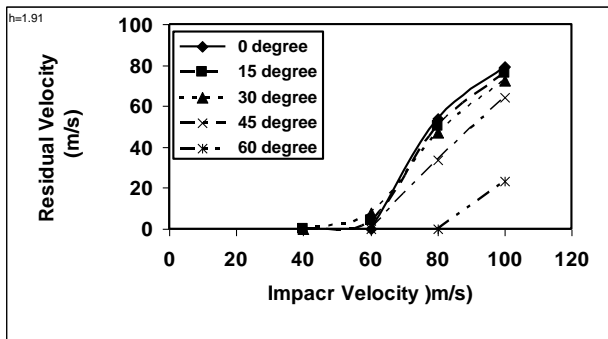


Fig.6. Residual versus impact velocity for 01.91 mm plate thickness with different obliquity angles (numerically)

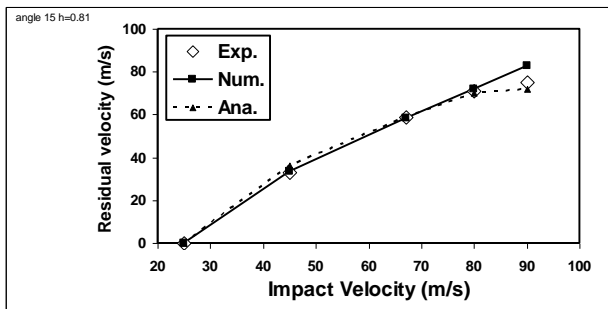


Fig.7. Comparison between experimental, numerical, and analytical (equation 6) residual velocity for 15° obliquity of 0.81 mm thicknesses of aluminum plate.

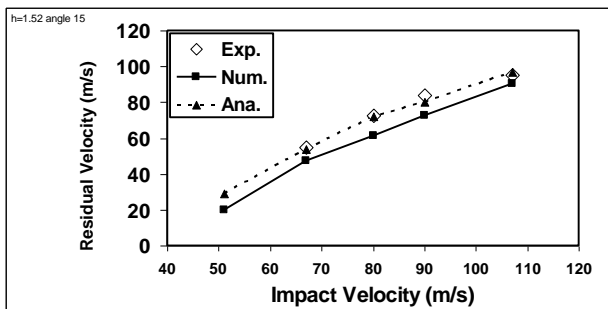


Fig.8. Comparison between experimental, numerical, and analytical (equation 6) residual velocity for 15° obliquity of 1.52 mm thicknesses of aluminum plate.

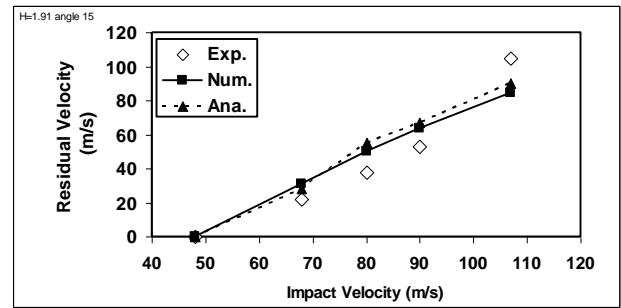


Fig.9. Comparison between experimental, numerical, and analytical (equation 6) residual velocity for 15° obliquity of 1.91 mm thicknesses of aluminum plate.

Figs. 7-9 show the computed, measured and analytical (equation 6) values of residual velocity at aluminum plate thicknesses for 15 degree obliquity angles are plotted against impact velocity.

Figs. 10-12 show the computed, measured and analytical (equation 6) values of residual velocity at all aluminum plate thicknesses for 30 degree obliquity angles are plotted against impact velocity.

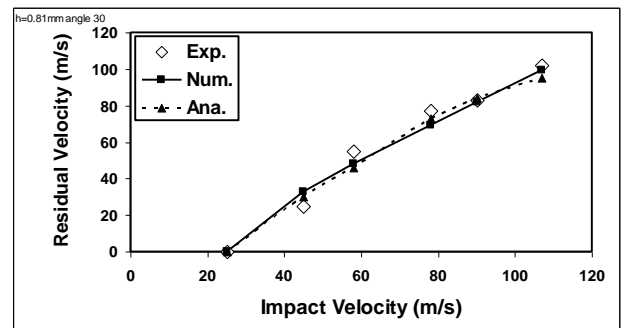


Fig.10. Comparison between experimental, numerical, and analytical (equation 6) residual velocity for 30° obliquity of 0.81 mm thicknesses of aluminum plate.

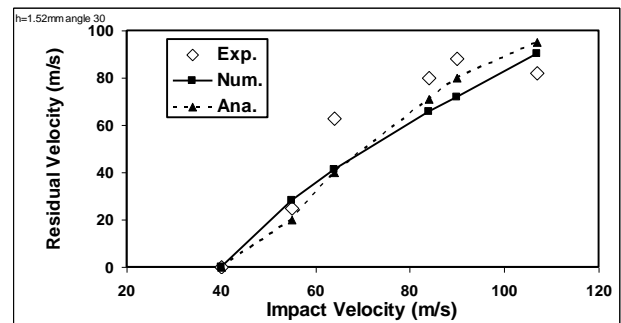


Fig.11. Comparison between experimental, numerical, and analytical (equation 6) residual velocity for 30° obliquity of 1.52 mm thicknesses of aluminum plate.

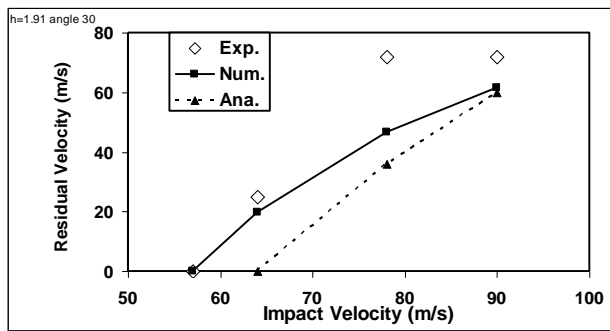


Fig.12. Comparison between experimental, numerical, and analytical (equation 6) residual velocity for 30° obliquity of 1.91 mm thicknesses of aluminum plate

5.3 Plate Thickness Influence (Angle Of Obliquity 15 Degree) On The Absorbed Energy

The effect of impact energy on the energy absorbed by the plates during perforation is shown in Figures 13-15, which illustrate the comparison for the computed, experimental and analytical results.

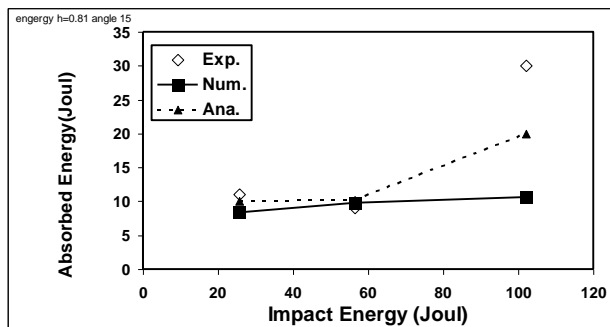


Fig.13. Comparison between experimental, numerical, and analytical (equation 4) absorbed velocity for 15° obliquity of 0.81 mm thicknesses of aluminum plate.

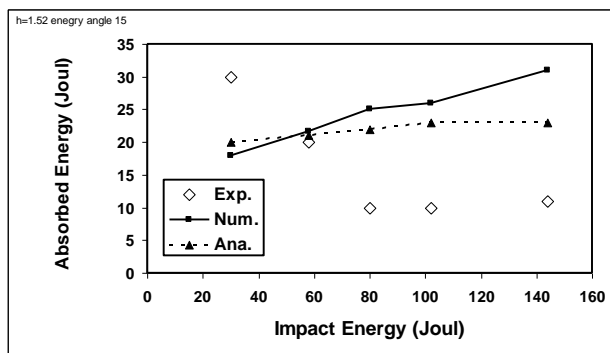


Fig.14. Comparison between experimental, numerical, and analytical (equation 4) absorbed velocity for 15° obliquity of 1.52 mm thicknesses of aluminum plate.

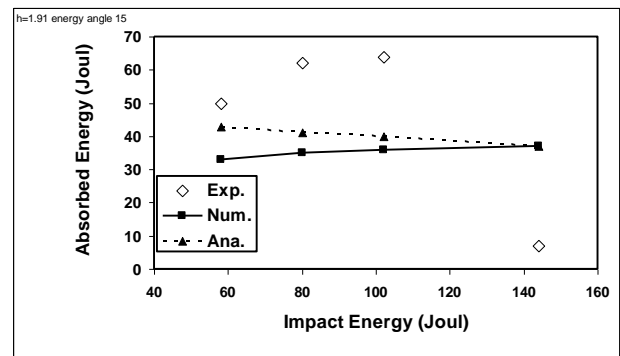


Fig.15. Comparison between experimental, numerical, and analytical (equation 4) absorbed velocity for 15° obliquity of 1.91 mm thicknesses of aluminum plate

5.4 Plate Thickness Influence (Angle Of Obliquity 30 Degree) On The Absorbed Energy

The effect of impact energy on the energy absorbed by the plates during perforation is shown in Figs 16-18.

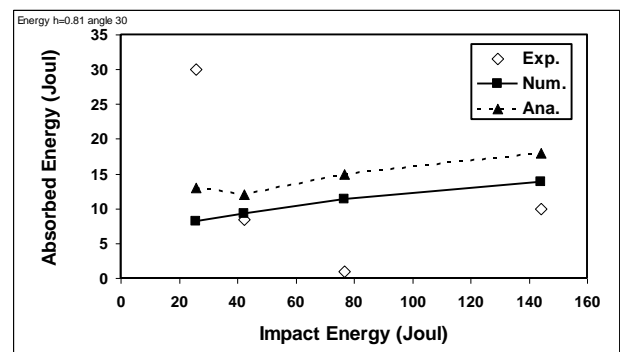


Fig.16. Comparison between experimental, numerical, and analytical (equation 4) absorbed velocity for 30° obliquity of 0.81 mm thicknesses of aluminum plate

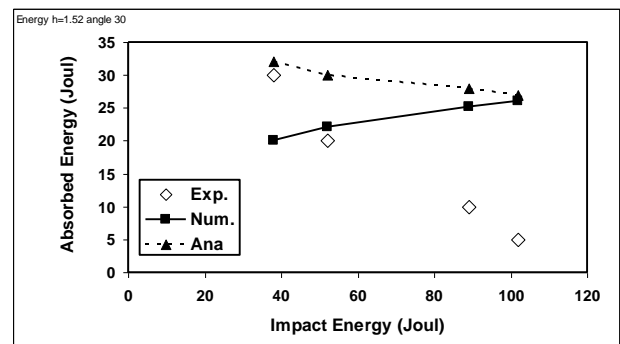


Fig.17. Comparison between experimental, numerical, and analytical (equation 4) absorbed velocity for 30° obliquity of 1.52 mm thicknesses of aluminum plate.

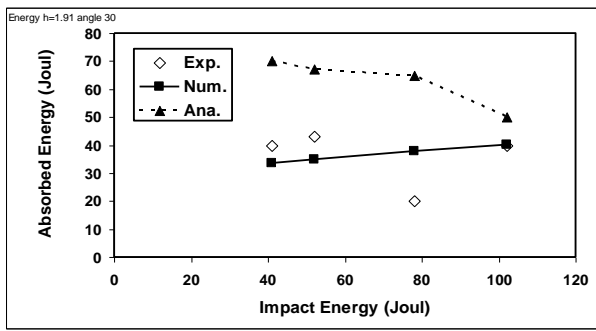


Fig.18. Comparison between experimental, numerical, and analytical (equation 4) absorbed velocity for 30° obliquity of 1.91 mm thicknesses of aluminum plate.

The absorbed energy by the aluminum plates during perforation has no significant variation at different impact energy levels of the projectile for plate thickness in the velocity range used. In general, the absorbed energy increases with an increase in aluminum plate thickness.

5.5 Effect of Obliquity

The computed values of the residual velocities are plotted against the impact velocities for a given plate thickness at different angles of obliquity are shown in Figures 19-23. The residual velocity, in general, decreases with increase in the angle of obliquity.

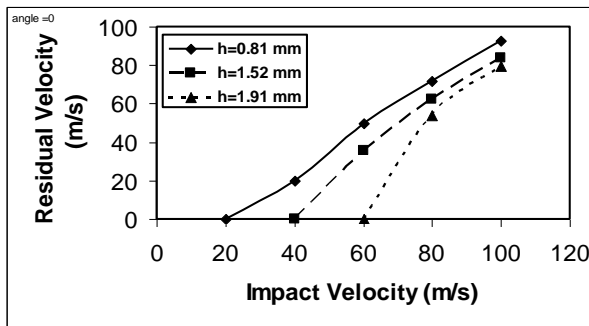


Fig.19. Numerical residual velocity for 0° obliquity for all plate thicknesses

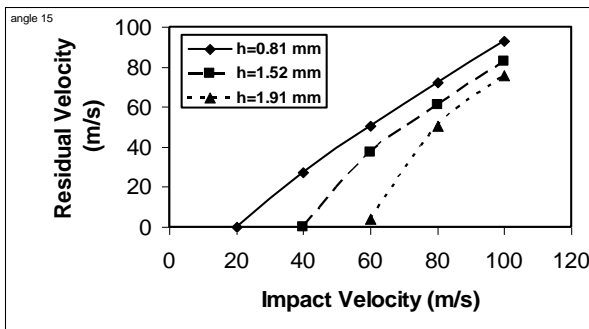


Fig.20. Numerical residual velocity for 15° obliquity for all plate thicknesses

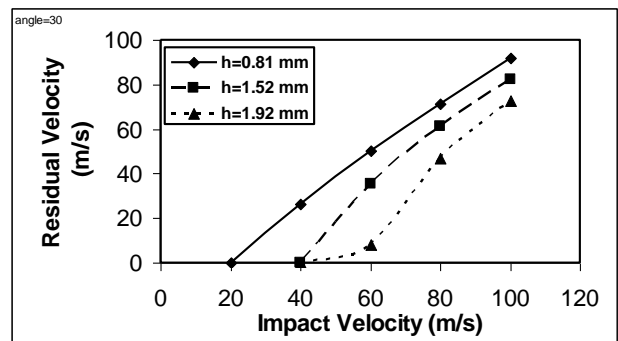


Fig.21. Numerical residual velocity for 30° obliquity for all plate thicknesses.

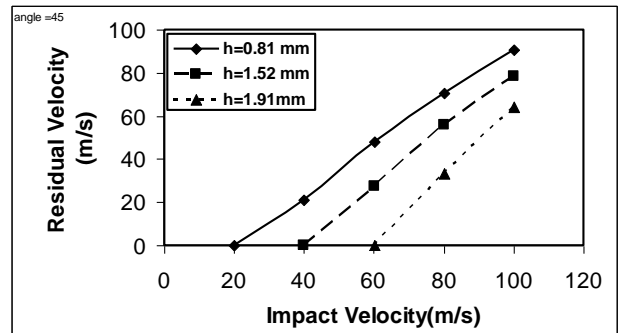


Fig.22. Numerical residual velocity for 45° obliquity for all plate thicknesses.

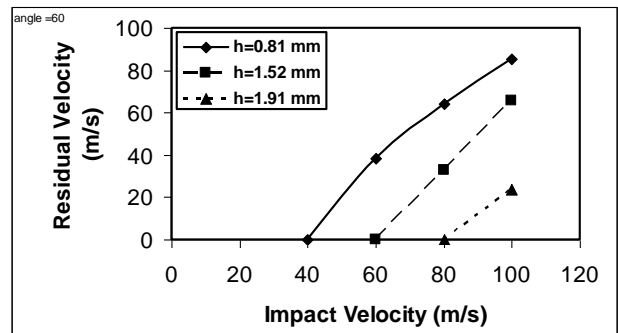


Fig.23. Numerical residual velocity for 60° obliquity for all plate thicknesses

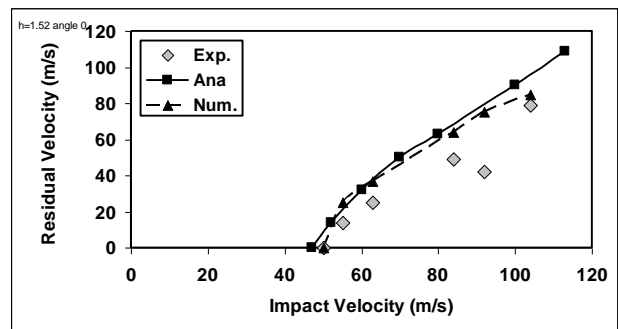


Fig.24. Comparison between the numerical, experimental and analytical (equation 6) residual velocity for 1.52mm plate thickness equal to 1.52 mm of 0° obliquity

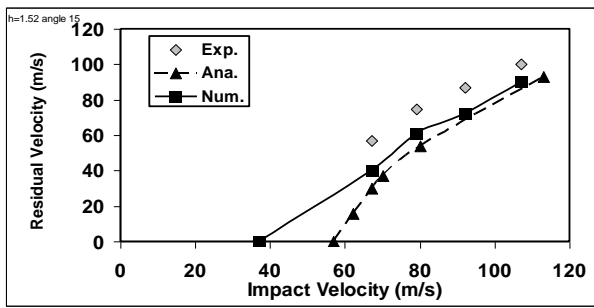


Fig.25. Comparison between the numerical, experimental and analytical (equation 6) residual velocity for 1.52mm plate thickness equal to 1.52 mm of 15° obliquity.

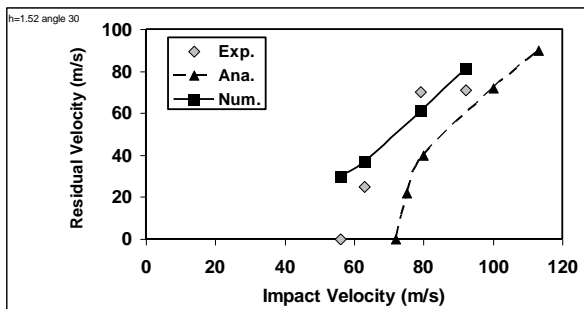


Fig.26. Comparison between the numerical, experimental and analytical (equation 6) residual velocity for 1.52mm plate thickness equal to 1.52 mm of 30° obliquity.

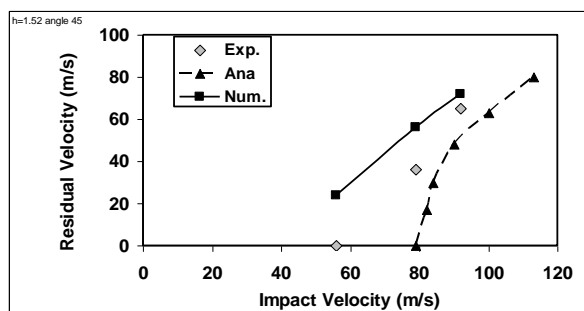


Fig.27. Comparison between the numerical, experimental and analytical (equation 6) residual velocity for 1.52mm plate thickness equal to 1.52 mm of 45° obliquity

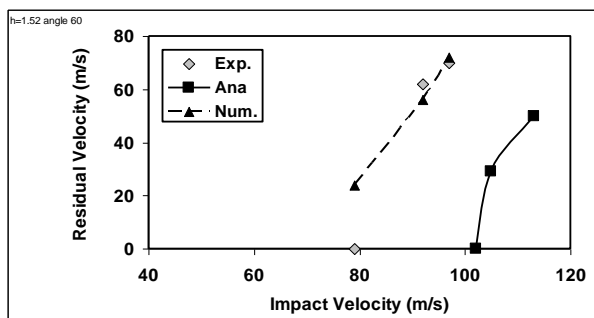


Fig.28. Comparison between the numerical, experimental and analytical (equation 6) residual velocity for 1.52 mm plate thickness equal to 1.52 mm of 60° obliquity

Figs. 24-28 show the comparison between the numerical, experimental and analytical results for aluminum plate

thickness equal to 1.52 mm for obliquity angles 0,15,30,45,and 60 degree.

6. FAILURE MODE

In normal impact and at low velocities (near the ballistic limit) the plate suffers bending with noticeable amount of deflection while this deflection decreases with increase of impact velocity, and perforation zone has a circular shape. With oblique impact the plate bending decrease with increase the oblique angle, and perforation zone has an ellipse shape. Figures (29-33) illustrate a model of the failure mode of the projectile impact on 0.81 mm aluminum plate thickness with different oblique angle.

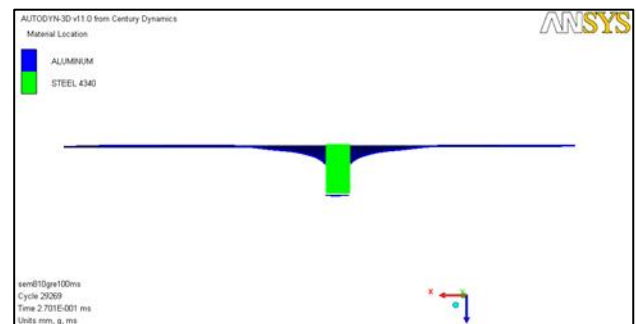


Fig.29. Numerical impact pair model with 0° obliquity

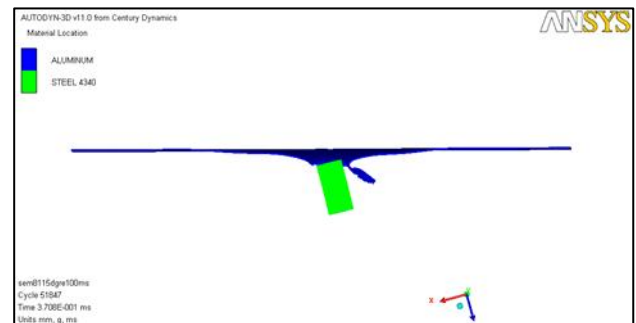


Fig.30. Numerical impact pair model with 15° obliquity.

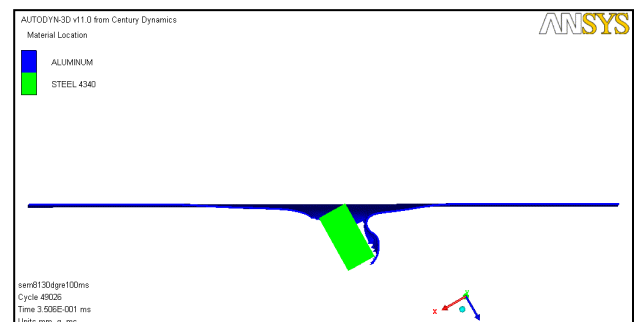


Fig.31. Numerical impact pair model with 30° obliquity

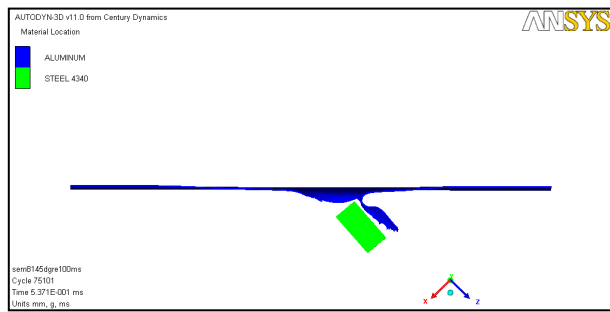


Fig.32 .Numerical impact pair model with 45° obliquity



Fig.33 .Numerical impact pair model with 60° obliquity

7. CONCLUSIONS

3D-Finite element simulations of normal and oblique impact of cylindrical steel projectile on different aluminum thicknesses plates have been performed using ANSYS-AUTODUN finite element code. The aluminum plate thickness and the obliquity angle have a significant effect of the residual velocities and on the absorbed energy by the plate during impact and perforation event. The numerical results have been compared with experimental and analytical results with good correlation

REFERENCES

- [1] J. Awerbuch, & S.R. Bodner, "Experiments on the normal perforation of projectiles in metallic plates," *Int. J. Solids Struct.*, 10, 685-99. 1974,
- [2] NK. Gupta, R. Ansari, and Gupta, SK. "Normal impact of ogival nosed projectiles on thin plates," *Int. J. Imp Eng*, 25, pp. 641-660. 2001.
- [3] NK. Gupta, MA. Iqbal, and GS. Sekhon, "Experimental and numerical studies on the behaviour of thin aluminium plates subjected to impact by blunt- and hemispherical-nosed projectiles." *Int. J. Imp Eng*, 32(12), pp. 1921-1944. 2006,
- [4] ME. Backman,, and W. Goldsmith," The mechanics of penetration of projectile into targets," *Int. J. Eng Sci*, 16, pp.1-99. 1978.
- [5] Gupta, NK., and Madhu, V. An experimental study of normal and oblique impact of hard-core projectile on

single and layered plates. *Int. J. Imp Eng*, 1997, 19, pp. 395-414.

- [6] WU. Khan, R. Ansari,, and NK. Gupta, "Oblique impact of projectile on thin aluminium plates," *J.Defence Science*, 58(2), pp. 139-146. 2003.
- [7] RSJ. Corran, PJ. Shadbolt,, and C. Ruiz," Impact loading of plates - An experimental investigation,". *Int.J.Imp Eng*, 1(1), pp.3-22. 1983.
- [8] T. Borvik, M. Langseth, OS. Hopperstad, and K.A. Malo," Perforation of 12 mm thick steel plates by 20 mm diameter projectiles with flat, hemispherical and conical noses: Part I: Experimental study," *Int. J.Imp Eng*, 27, pp. 19-35. 2002.
- [9] Fawaz, Z., Zheng, W., and Behdinin. K. Numerical simulation of normal and oblique ballistic impact on ceramic composite armours. *Comp Struct*, 2004, 63, pp. 387-395.
- [10]Kad, BK., Schoenfeld, SE., and Burkins, MS. Through thickness dynamic impact response in textured Ti-6Al-4V plates. *Mat. Sci and Eng A*, 2002, 322, pp. 241-251
- [11]T. Borvik, M, Langseth, OS. Hopperstad, and K.A. Malo," Perforation of 12 mm thick steel plates by 20 mm diameter projectiles with flat, hemispherical and conical noses: Part II: Numerical study," *Int. J. Imp Eng*, 27, pp. 37-64. 2002.
- [12]CT. Lim, VPW. Shim, and Ng, YH. "Finite-element modelling of the ballistic impact of fabric armour,"*Int. J. Imp Eng*, 28, pp. 13-31. 2003.
- [13]VBC. Tan, CT. Lim, and CH. Cheong," Perforation of high strength fabric by projectiles of different geometry," *Int. J. Imp Eng*, 28, pp. 207-222. 2003.
- [14]D. Nandlall, K. Williams,, and R. Vaziri,"Numerical simulation of the ballistic response of GRP plates," *Comp Sci and Tech*, 58, pp. 1463-1469. 1998.
- [15]M. Park,, J. Yoo,, and D-T. Chung," An optimisation of multi-layered plate under ballistic impact," *Int. J.Solids and Struc*, 42, pp. 123-137. 2005.
- [16]C.A. Calder, & W. Goldsmith, "Plastic deformation and perforation of thin plates resulting projectile impact," *Int. J. Solids Struct.*, 7, 863-881. 1971.
- [17]N.K. Gupta, R. Ansari, & S.K. Gupta," Normal impact of ogive-nosed projectiles on thin plates," *Int. J. Impact. Engg.*, 25, 641-660. 2001.